Asian Journal of
Science, Technology, Engineering, and Art

e-ISSN: 3025-4507
p-ISSN: 3025-5287
Index: Harvard, Boston, Sydney University, Dimensions, Lens, Scilit, Semantic, Google, etc

https://doi.org/10.58578/AJSTEA.v3i2.4921

Load Frequency Control (LFC) Strategy for an Isolated Microgrid Integrated with Electric Vehicles

A.D. Chun[1], S. B. Visa[2], I. H. Charles[3], Rufai Hassan[4], S. C. Gasin[5]
[1,2,3,4]Ahmdu Bello University, Zaria, Nigeria; [5]Federal Polytechnic Bali, Taraba State, Nigeria
adChun@abu.edu.ng; sbvisa@abu.edu.ng

Article Info:

Submitted:	Revised:	Accepted:	Published:
Jan 5, 2025	Jan 20, 2025	Feb 2, 2025	Feb 7, 2025

Abstract

The growing demand for efficient and sustainable energy solutions has driven the widespread adoption of Distributed Energy Resources (DERs) and microgrids. However, the intermittent nature of DERs and the low inertia of isolated microgrids present significant challenges for Load Frequency Control (LFC). Primary frequency control alone often fails to maintain system frequency within acceptable limits. To address this issue, this research proposes an LFC strategy for a hybrid standalone microgrid (SMG) leveraging electric vehicles (EVs). The approach incorporates a Proportional-Integral-Derivative (PID) controller in the SMG design model. The objective function is formulated using the Integral of Time-Weighted Absolute Error (ITAE), and the Particle Swarm Optimization (PSO) algorithm is employed to optimize the PID gain parameters. Furthermore, Flywheel Energy Storage System (FESS) and Battery Energy Storage System (BESS) components are integrated with the PID controller's output to enhance LFC performance. The system capitalizes on the high-energy density and bidirectional charging/discharging capabilities of EVs to effectively regulate frequency variations. The effectiveness of the proposed method is validated through three simulation scenarios. In Scenario 1, the proposed technique achieves a 61.82% improvement in frequency

deviation and a 40% reduction in settling time. Scenario 2 shows further enhancement, with improvements of 78.26% in frequency deviation and 61.54% in settling time. The simulation results consistently demonstrate that the proposed technique outperforms existing methods across all scenarios in terms of frequency deviation and settling time improvements.

Keywords: Load Frequency Control; isolated Microgrid; Particle Swarm Optimization; Electric Vehicles

INTRODUCTION

The rising demand for efficient and sustainable energy use has resulted in the extensive implementation of Distributed Energy Resources (DERs) and micro-grids (Nzoundja et al., 2025). The adoption of renewable energy sources (RESs) like solar, wind, or biofuels, along with their incorporation into traditional power grids, has been escalating daily due to the swift depletion of fossil fuels, heightened environmental pollution issues, and rising energy demands (Inderjeet, 2023). Standalone microgrid with controllable distributed generations have slow dynamic response, resulting from low system inertia, non-linear structure and intermittent nature of the distributed energy resources (DERs). However, the intermittent nature of power generation from renewable resources, combined with load variations, can cause imbalances between supply and demand, leading to frequency fluctuations (Ranjan & Shankar, 2024). The most substantial issues with Standalone MGs are variations in output power of RES which depend on wind speed, and Solar irradiance, these can lead to significant frequency fluctuations and may even result in a system failure. In islanded mode, power imbalances cannot be addressed by the upstream network, unlike the grid-connected mode. This can lead to serious frequency instability and power quality issues. Therefore, an effective frequency control strategy is essential to manage these uncertainties, disturbances, and dynamic variations. (Aff et al., 2023).

Earlier frequency control scheme used flyballs to activate a hydraulic system by adjusting the throttle valves of the system prime movers. Modern generators use electronic governors to accomplish the same (Kunya, 2024). Several approaches are applied to reduce damping effect and large frequency fluctuations caused by non-inertial RES on LFC in standalone microgrid and sudden load variations (Khazali et al., 2022).

Load frequency control mechanism is essential for maintaining grid stability by adjusting generation output to match variations in real-time. The primary objective of controlling the Load Frequency in a microgrid is to sustain zero variation in frequency of islanded mode, accurately track load changes and disturbances, minimize settling time, and determine the maximum undershoot and overshoot values during frequency deviations (Alayi et al., 2021). The primary control is deployed to stabilize frequency and ensure effective load sharing among Distributed Generators (DGs). Controllable Distributed Generators (DGs) are installed in standalone microgrids (MGs) to increase the system's inertia constant. However, these DGs have a slow dynamic response, which limits their ability to adequately support primary frequency control. To address this, highly efficient Battery Energy Storage (BES) devices with fast dynamic response are widely used to provide the necessary frequency support (Hasan et al., 2024).

Literature Review

A microgrid is a localized, low-voltage distribution network that ensures a stable electrical supply within a defined area (Kostenko & Zaporozhets, 2023). It consists of distributed generators (DGs), energy storage systems (ESSs), loads, and control devices. Microgrids can operate in two modes: grid-connected mode, where the microgrid interacts with the main utility grid by absorbing or delivering power, and islanded mode, where the microgrid operates independently, autonomously supplying power to local loads (Ghelani, 2022).

Microgrids are categorized based on application and structure into AC, DC, or hybrid AC/DC systems and serve both remote and urban areas (Aljafari et al., 2022). A hybrid microgrid integrates AC and DC-based distributed energy resources (DERs), ESSs, and loads into the existing distribution system (Abdelwanis et al., 2024). From a utility perspective, a microgrid functions as a single controllable entity capable of responding rapidly to transmission system needs. For consumers, it ensures reliable, efficient, and uninterrupted power while reducing feeder loss, improving local voltage support, and increasing overall efficiency (Khan et al., 2024). Integration into the main grid provides additional benefits such as pollution-free, cost-effective, and sustainable energy (Ramesh et al., 2020).

Electric Vehicles.

An Electric Vehicle (EV) is a mobile energy storage unit that integrates various subsystems, working together for propulsion. EVs can run solely on electric power or have an Internal Combustion Engine (ICE) operating alongside. Basic EVs use only batteries, while hybrid EVs (HEVs) utilizes additional energy sources. According to the International Electrotechnical Commission (IEC), HEVs must be equipped with two or more energy sources, storage systems, or converters. with at least one providing electrical energy (Un-Noor *et al.*, 2017).

Frequency Control in Microgrid

In Islanded microgrids, a high integration of renewable energy sources can cause frequency fluctuations, disrupting stability in power system operation. Battery energy storage systems are commonly employed to regulate these variations and maintain stability. Frequency plays a key role in ensuring the microgrid's reliability and power quality. Maintaining frequency stability is essential for ensuring source-load balance and effectively redistributing active power.(Liu *et al.*, 2020).

PID Controller

Described by a second order differential equation, this controller has a wide range of functionality mostly because of its simplicity of implementation, used majorly in process industries, it is a combination of three terms/parts: Proportional, integral and derivative terms, each has a gain that is adjustable to achieve a desired effect on the controlled plant. The proportional gain k_p subject to the current error, integral gain k_i subject to the accumulated error and the derivative gain k_d depends on predicted future error. The controller's output is the sum of the three gains. k_p, k_i, k_d.

The choice of PID controller in this work is because it has the ability to correct errors in a control system which is why it is sometimes referred to as a compensator. PID controller design is adapted from(Humusoft 1996-2008).

$$G_r(s) = k_p + \frac{k_i}{s} + k_d s \tag{1}$$

Optimization of LFC Parameters

This research employed proportional-integral-derivative (PID) controllers to regulate the frequency of a standalone microgrid. The PID controllers serve as the LFC Supplementary Controller, a PID controller is designed to achieve an optimal control scheme with improved closed loop performance, the PID controller gains (K_P, K_i and K_d) will be optimized through the Particle Swarm Optimization (PSO) algorithm, with the objective of minimizing the performance index (J_p) based on the Integral Time Absolute Error criterion given by:

$$ITAE = \int_0^{t_{Sim}} t.|\Delta f|dt \quad (2)$$

Particles Swarm Optimization (PSO)

Particle swarm algorithm is a populace based stochastic streamlining strategy that imitates the conduct of the flock of birds or school of fish, Ebert and Kennedy (1995). The framework is initiated using a population of random particles, followed by the optimization search. The potential arrangements called particles fly through the issue space by following the present ideal particles. Every molecule keep space which are related with the best arrangement it has accomplished so far that is called P_{best}, when a particle considers all particles as its topological neighbors, the best value found is known as the global best, or Gbest. In PSO, each particle updates its velocity based on its personal best (Pbest) and the global best (Gbest) positions. (Kumarakrishnan *et al.*, 2020).

PSO uses two main equations to update each particle's velocity and position, defined respectively as given in

$$v_{i+1}{}^k = \omega v_i^k + c_l r_l\left(d_{best}^k - d_i^k\right) + c_g r_g\left(G - d_i^k\right) \quad (3)$$

where ω is the inertia weight, $c_l$and cg are acceleration parameters representing self

Materials And Methods

The materials and methods were adopted and used in designing and simulating SMG model for controlling load frequency.

Designing the Standalone Micro Grid Model

The design of the SMG was actualized by the following steps:

(1) Determine the model of the renewable energy sources and non-renewable energy sources for the SMG. (2) Also, obtaining the transfer function for the governor, turbine and generator respectively. (3) Next, connecting the FESS and BESS transfer function blocks to the output of the PID controller. (4) In addition, the feedback loop was connected as input to the PID controller. (5) Furthermore, the ITAE design the Simulink was designed and was linked with the objective function of the PSO algorithm. (6) Finally, the gain parameters of the PID controller were determine by the objective function of the PSO code in the MATLAB environment. The above-mentioned steps for the design of the SMG model are explained below:

(2) **Obtaining the Individual Blocks for the Renewable and Non-Renewable Sources.**

By obtaining the individual models for the renewable energy source. The renewable sources are PV and WTG:

The Renewable Energy Sources (PV and WTG): In the Simulink environment; Go to the library browser and select Simscape to obtain the PV block and WTG block. In the Simulink library browser, in the search results, select Simulink, in Simulink dropdown, select commonly used blocks, select continuous, in continuous blocks, select transfer Fcn block and insert the values for the transfer function for the PV and WTG sources. The values for the transfer function for the renewable sources are gotten from Table 1 respectively

DEG Model: Go to the Simulink library browser, in the search results, select Simulink, in Simulink dropdown, select commonly used blocks, in commonly used block dropdown, select continuous, in continuous blocks, select transfer Fcn block and insert the values for the transfer function for DEG. Also, in Simulink dropdown, select commonly used blocks in commonly used blocks

EV Model: In the Simulink environment, go to Simulink library browser, in the search results, select Simulink, in Simulink dropdown, select commonly used blocks, in commonly used block dropdown, select continuous, in continuous blocks, select transfer Fcn block and insert the values for the transfer function for EV. Also, in Simulink dropdown, select commonly used blocks in commonly used blocks drop down, select saturation and insert the values. Likewise, in the Simulink dropdown, select commonly used blocks, in

commonly used block dropdown, select constant block, summation block, integrator block, gain block and switch block. The values for the blocks are in Table 1 respectively.

Calculating the Values of the Energy Capacity Limit of the EV

The values for $N_{control}$ and C^*_{kWh} are obtained from Table 1

$N_{control}$ = 82,

C^*_{kWh}= 15

Lower energy capacity limits for the EV

$$E^{min}_{control} = \frac{82\times15}{1000} \times 0.8 = 0.984$$

Upper energy capacity limit for the EV

$$E^{max}_{control} = \frac{82\times15}{1000} \times 0.9 = 1.107$$

Obtaining the Transfer Function for the Governor, Turbine and Generator

Go to the Simulink library browser, in the search results, select Simulink, in Simulink dropdown, select commonly used blocks, in commonly used block dropdown, select continuous, in continuous blocks, select transfer Fcn block and insert the values for the transfer function for the Governor, Turbine and Generator. The values for the transfer function of the Governor, Turbine and Generator are in Table 1 respectively.

Connecting FESS and BESS to the Output of the PID Controller

The transfer function blocks of the BESS and FESS are connected to the output of the PID controller as shown in Figure 1 against being connected to the output of the transfer function of the system load.

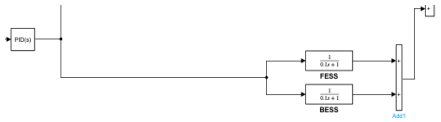

Figure 1: Connecting FESS and BESS to the PID out

Connecting the feedback loop as input to the PID controller

The feedback loop with a gain block was connected to the input to the PID controller through a sum block as shown in Figure 2.

Figure 2: Connecting the feedback loop as input to the PID controller ITAE

Model Design and Linked with the Objective Function of the PSO Algorithm

The ITAE model was design by the following steps:

(i) From equation 2 the ITAE model was design in Simulink design software. Go to library browser and click on math Operations then select Abs and product block. Similarly, in the library browser, click on Simulink and select integrator block. Also, in the library browser, click on Simulink and select sources and chose the clock block. Furthermore, in Simulink library browser, click on Simulink and in the Simulink dropdown, select sinks and in sink dropdown select display block. and 'To workspace block' respectively.

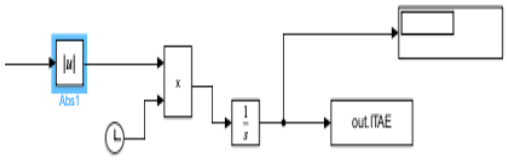

Figure 3: Integral Time Absolute Error Model

(ii) Connecting c to the PID controller input.

The ITAE input is connected to the PID controller's feedback loop to measure load frequency deviation in the system, as shown in Figure 5.

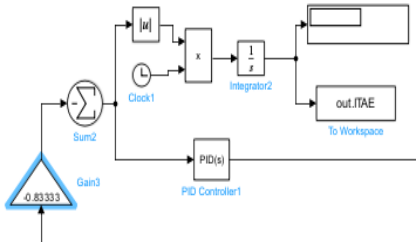

Figure 4: Connecting ITAE to the Output of the PID Controller

Determine the PID Gain Parameters for the Design

Click on Simulink, select continuous in continuous dialog box select PID controller block

Set the PID gains to variable KK1, KK2 and KK3 respectively.

Connecting the SMG Simulink model to MATLAB environment using to workspace block.

The objective function **(f_{obj})** of the PSO is the minimize load frequency deviation error

$$f_{obj} = ITAE = \int_0^\infty t.|e(t)|dt \quad (4)$$

Then, run the PSO code to tuning the PID gain parameters to obtain the optimal gain parameters. The realized values for the tuning the PID gain parameters after running the PSO codes are as follows:

Proportional Gain (K_P) :1000

Integral Gain (K_I) :1000

Derivative Gain (K_D): 0

The realized values for the PID gain parameters K_P, K_I and K_D are replaced with the PID gains variables KK1, KK2 and KK3 in the PID controller block in the SMG Simulink model.

KK1= K_P = 1000

KK2 = K_I = 1000

KK3 = K_D = 0

Before carrying out simulation on the SMG model in the Simulink environment to obtain the result on load frequency deviation in the scope.

Figure 5 showed the developed Simulink model of the design of the improved Standalone Micro Grid (SMG) model is shown in Figure 5. The designed SMG comprises of a renewable and non-renewable energy sources PV, WTG and EV, DEG. It also made up of a transfer function of the governor, turbine and generator linked with a summation block with the above mention energy sources. The FESS and BESS are connected to the output of the PID controller. The feedback loop was connected as input to the PID controller, as well as the ITAE Model. The ITAE Model was linked with the objective function of the PSO algorithm with the aid of 'To workspace block.

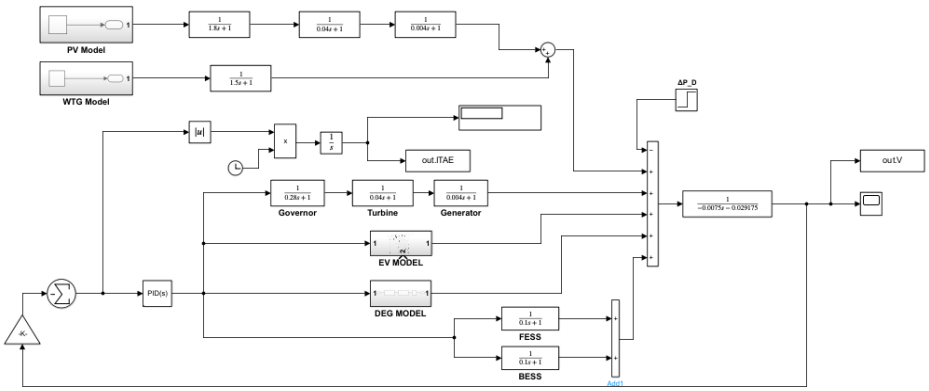

Figure 5: Simulink Model of the Improved SMG System

Table 1. Simulation parameters

Symbol	Parameters	Values
2H	Inertial constant of the MG.	0.1167 s
D	Load damping coefficient	0.015
T_T	Turbine time constant	0.01 s
T_G	Governor time constant	0.4 s
T_{IN}	Inverter time constant	0.04 s
F	Nominal frequency	60 Hz
Tic	Interconnector time constant	0.004 s
T_{FC}	FC time constant	0.28 s
K_{FC}	FC gain	1
T_{BESS}	BESS time constant	0.1 s
T_{FESS}	FESS time constant	0.1 s
R	Governor speed regulation coefficient	2.4 Hz/pu
T_{WTG}	WTG time constant	MW
K_{WTG}	WTG gain	1.5 s
T_{PV}	PV time constant	1
K_{PV}	PV gain	1.8 s
T_{EV}	EV time constant	1
C^*_{kW}	Inverter capacity of the EV energy storage system	1 s
C^*_{kW}	Inverter capacity of EV energy storage system per h	3
C^*_{kWh}	Inverter capacity of EV energy storage system per h	15
$N_{control}$	Number of controllable Evs	82

RESULTS

The Proposed controller was implemented in the single-area LFC system with EVs. After applying the proposed techniques, the system was subjected to step load perturbation

(SLP), comparative ITAE convergence characteristics and Variation in system parameters, this will be further explained in details in the subsection below.

Simulation Results of the Proposed-PID and PI-PD Considering Scenario 1

Scenario 1: Subjection of SMG to 1% SLP at constant ΔP_{WTG} and ΔP_{PV} with EV inclusion. When the system was subject to 1% step load perturbation keeping ΔP_{WTG} and ΔP_{PV} constant and EV was incorporated, the result obtained is as shown in the Figures 6, the first scenario, In this, the SMG system was subjected to 0. 01p.u step load perturbation with ΔP_{WTG} and ΔP_{PV} maintained constant, as depicted in Figure 6. Considering the reduction in frequency oscillation, it is evident that the proposed PID controller (with EV inclusion) demonstrated superior dynamic performance by damping the frequency oscillation (undershoot) to 0.00042 p.u. Hz, as shown in Figure. This performance is significantly better compared to the existing PI-PD controller (with EV inclusion). As shown in Table 2, the frequency deviation (undershoot) and the settling time were both reduced when the proposed PID controller (with EV) was applied. The results indicate that the frequency deviation (undershoot) and the settling time of the system achieved percentage improvements of 61.82% and 40%, respectively, using the proposed technique.

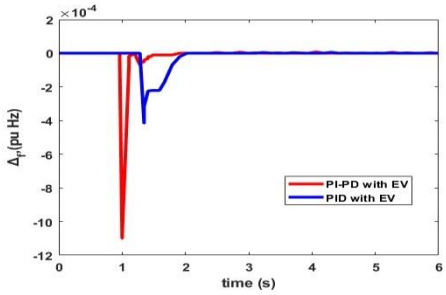

Figure 6: Load Frequency Deviation against Time

Figure 7 shows ITAE convergence curves for SSO (with EV) and PSO (with EV). From the Figure, it was observed that, the proposed PSO (with EV) demonstrates a significant improvement over SSO (with EV) in terms of optimizing the performance index as shown from Figure 7. From the convergence curve in Figure 8, the PSO (with EV) converges more quickly and reaches a much lower performance index value of 0.000005 at 7th iteration, therefore, the proposed technique is more effective at finding a better solution or achieving better optimization than SSO. With this lower performance index achieved, efficient use of generation sources, storage, and loads, minimizing fuel consumption is obtained.

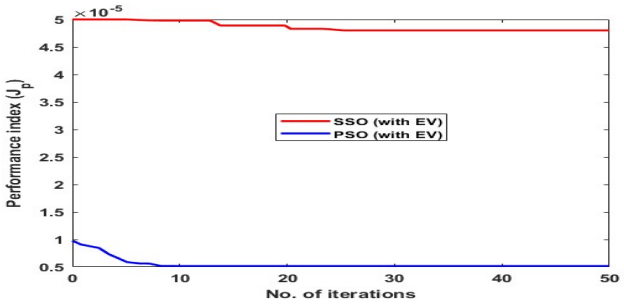

Figure 7: ITAE convergence curves for SSO (with EV) and PSO (with EV).

Simulation Results of the Proposed-PID and PI-PD Considering Scenario 2.

The results obtained for the Subjection of SMG to 1% SLP at constant ΔP_{WTG} and ΔP_{PV} without EV inclusion:

Figure 8 shows the simulation for SMG frequency response. In this, immediately after the 0.01 p. u step load perturbation was applied, the proposed controller shows a superior transient stability and faster recovery from perturbations as shown in figure. In table 2, It is evident that utilizing the proposed PID controller in the MG structure, improve the steady state response. The Proposed PID controller provides better damping of oscillations with and a quicker return to a steady-state frequency compared to the PI-PD controller. The comparative analysis from table 2 proves that the proposed techniques without EV is superior over the existing controller with ,66.67%,78.26% and 61.54% in times of Overshoot (O_{sh}),Undershoot (U_{sh})and settling time (T_s) improvement respectively.

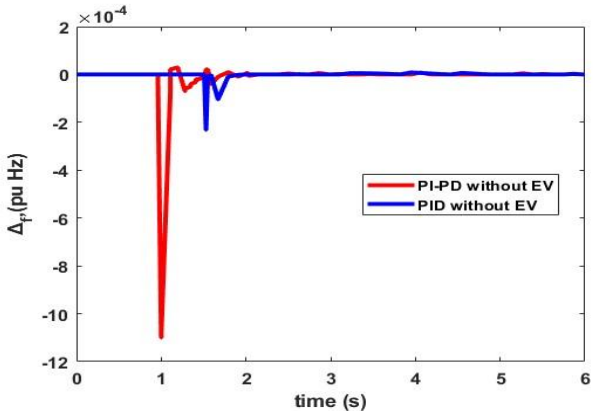

Figure 8: shows Time Domain simulation for SMG frequency response

Figure 9: shows the ITAE convergence curves for SSO (without EV) and PSO (without EV). It was observed from the Figure that, while searching for the optimum controller gain, PSO (without EV) was able to obtain best cost function of 0.0000006 at the 3rd

iteration. The curve depicts that the PSO algorithm converges faster than SSO and has achieved a lower value of the performance index showing better optimization results compared to SSO. PSO is more effective at finding an optimal solution in this scenario without electric vehicles.

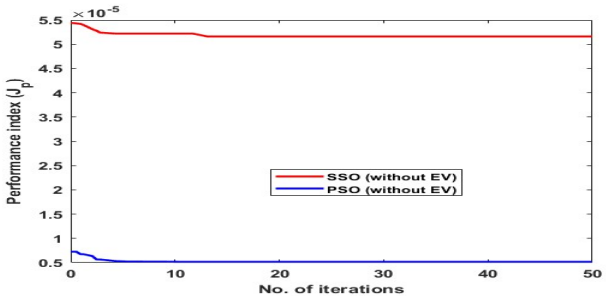

Figure 9: ITAE convergence curves for SSO (without EV) and PSO (without EV)

Figure 10 shows time domain simulations of the SMG under -50% parameter values variations. It was that when the system is subjected to -50% variations in the values of D, H, and R, the proposed technique demonstrates better robustness to parameter variation as seen from the figure 10. This pattern is magnified in the inset figure on the left of figure 10. The left inset zooms in on the blue curve in figure 10, revealed that the proposed PID controller has, faster damped oscillations. From Table 2 PID Controller shows better handling of the system variations with a percentage improvement in frequency deviation and settling time as 74.12% and 84.48% respectively. This suggests that PID controller is more suitable for microgrid LFC applications where parameter variations are likely to occur.

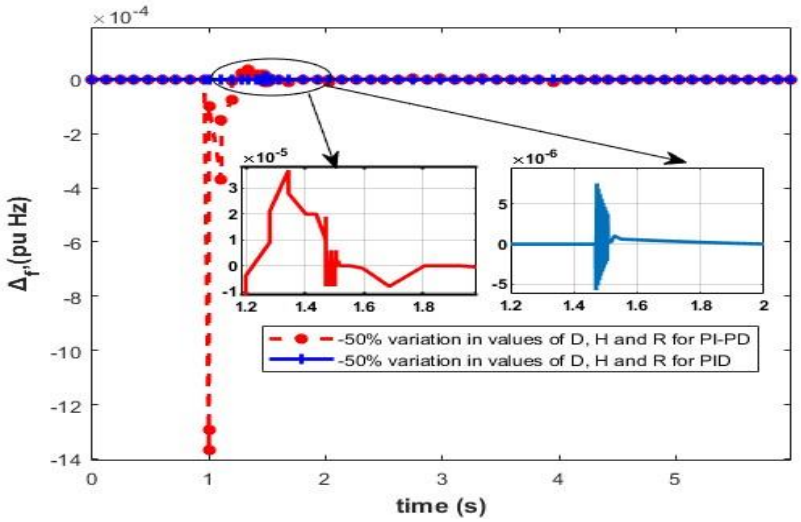

Figure 10: Time domain simulations of the SMG under -50% parameter values variations

Performance Comparison of the Proposed PID-Based and PI-PD-Based Controllers

The performance of the controllers was evaluated based on settling time and frequency deviation. The comparison focused on the proposed PID controller and the PI-PD controller for Load Frequency Control (LFC) in a hybrid standalone microgrid integrated with Electric Vehicles (EVs). The effectiveness of the proposed PID controller in the SMG design model is summarized in Table 2, highlighting its superior performance in achieving improved settling time and reduced frequency deviation compared to the PI-PD controller.

Table 2. Performance Comparison between the Proposed-PID and PI-PD Schemes

Performance Specification	**Controller**		**Percentage Improvement (%)**
	Proposed-PID	**PI-PD**	
Settling Time(seconds)	0.09	0.58	84.48
Frequency Deviation (Hz)	0.0000075	0.000029	74.14

DISCUSSION

The comparative analysis between the proposed PID controller and the PI-PD controller, as outlined in existing literature, highlights significant advancements in performance. Both controllers were designed to meet the critical specification of achieving a settling time of less than 1 second, an essential requirement for ensuring the stability of Load Frequency Control (LFC) systems in hybrid standalone microgrids integrated with Electric Vehicles (EVs).

The proposed PID controller demonstrated superior performance, achieving a 74.14% reduction in frequency deviation, effectively minimizing oscillations and enhancing frequency stability during dynamic disturbances such as step load perturbations. Additionally, the proposed controller reduced the settling time by 84.48%, ensuring a quicker return to steady-state conditions, thereby improving overall system responsiveness.

These results underscore the advanced capabilities and robustness of the proposed PID controller compared to the PI-PD controller referenced in prior research. By delivering enhanced stability and faster recovery, the proposed approach effectively meets the complex requirements of modern hybrid microgrids, establishing itself as a reliable solution for maintaining system performance across a range of operating conditions.

CONCLUSION

In this research work, the design and simulation of a Hybrid Standalone Microgrid (SMG) integrated with Electric Vehicles (EVs) were conducted. A PID controller was developed to stabilize the Hybrid Standalone Microgrid system, with load frequency control designed using proportional-integral-derivative methods and Particle Swarm Optimization (PSO) utilized to determine optimal controller parameters. The developed controller was simulated on a Standalone Microgrid model, and its performance was compared with an existing controller from the literature. The analysis revealed that the proposed technique achieved a faster settling time, improving by 84.48%, and exhibited a better frequency deviation response, with an enhancement of 74.14%. Overall, the designed controller demonstrated significant improvements in both frequency deviation and settling time across all tested scenarios. Based on these results, it is recommended that future studies focus on testing the modified model under more diverse operating conditions to enhance its robustness against extreme parameter variations and expand the scope to address multi-area systems, as the current study focused on a single-area system.

REFERENCES

Abdelwanis, M. I., & Elmezain, M. I. (2024). A comprehensive review of hybrid AC/DC networks: insights into system planning, energy management, control, and protection. *Neural Computing and Applications*, *36*(29), 17961-17977.

Aff, A., Simab, M., Nafar, M., & Mirzaee, A. (2023). Robust linear parameter varying frequency control for islanded hybrid AC/DC microgrids. *Electric Power Systems Research*, *214*,108898.

Alayi.R., Zishan.F.& Seyednouri S.R. (2021). Optimal Load Frequency Control of Island Microgrids via a PID controller in the presence of Wind Turbine and PV.13, (19), 10728.

Aljafari, B., Vasantharaj, S., Indragandhi, V., & Vaibhav, R. (2022). Optimization of DC, AC, and hybrid AC/DC microgrid-based IoT systems: a review. *Energies*, *15*(18), 6813.

Ghelani, D. (2022). LITERATURE REVIEW ON Coordinated Control of Interconnected Microgrid and Energy Storage System Dipteben Ghelani. *Authorea Preprints*.

Hasan, A. K., Haque, M. H., & Aziz, S. M. (2024). Enhancing Frequency Response Characteristics of Low Inertia Power Systems Using Battery Energy Storage. *IEEE Access*.

Inderjeet, M. (2023). *Fuel transition from non-renewable to renewable for gas turbines in a changing Europe* (Doctoral dissertation, Technische Hochschule Ingolstadt).

Khan, M. R., Haider, Z. M., Malik, F. H., Almasoudi, F. M., Alatawi, K. S. S., & Bhutta, M. S. (2024). A comprehensive review of microgrid energy management strategies considering electric vehicles, energy storage systems, and AI techniques. *Processes*, *12*(2), 270.

Khazali, A., Rezaei, N., Saboori, H., & Guerrero, J. M. (2022). Using PV systems and parking lots to provide virtual inertia and frequency regulation provision in low inertia grids. *Electric Power Systems Research*, *207*, 107859.

Kostenko, G., & Zaporozhets, A. (2023). Enhancing of the power system resilience through the application of micro power systems (microgrid) with renewable distributed generation. *System Research in Energy*, (3 (74)), 25-38.

Kunya, A. B. (2024). Hierarchical bi-level load frequency control for multi-area interconnected power systems. *International Journal of Electrical Power & Energy Systems*, *155*, 109600.

Liu, Y., Wang, X., & Wang, S. (2020). Research on frequency control of islanded microgrid with multiple distributed power sources. *Processes*, *8*(2), 193.

Nzoundja Fapi, C. B., Touré, M. L., Camara, M. B., & Dakyo, B. (2025). Control Strategy for DC Micro-Grids in Heat Pump Applications with Renewable Integration. *Electronics*, *14*(1), 150.

Ramesh, M., Yadav, A. K., & Pathak, P. K. (2021). Intelligent adaptive LFC via power flow management of integrated standalone micro-grid system. *ISA transactions*, *112*, 234-250.

Ranjan, M., & Shankar, R. (2024). Improved frequency regulation in smart grid system integrating renewable sources and hybrid energy storage system. *Soft Computing*, 1-20.